

5-2-2007

Development of a Capacitive Probe to Investigate Surface Charge on Gravitational-Wave Detector Optics

Robert McKinney
Trinity University

Follow this and additional works at: http://digitalcommons.trinity.edu/physics_honors



Part of the [Physics Commons](#)

Recommended Citation

McKinney, Robert, "Development of a Capacitive Probe to Investigate Surface Charge on Gravitational-Wave Detector Optics" (2007). *Physics & Astronomy Honors Theses*. 4.
http://digitalcommons.trinity.edu/physics_honors/4

This Thesis open access is brought to you for free and open access by the Physics and Astronomy Department at Digital Commons @ Trinity. It has been accepted for inclusion in Physics & Astronomy Honors Theses by an authorized administrator of Digital Commons @ Trinity. For more information, please contact jcostanz@trinity.edu.

Development of a Capacitive Probe to Investigate Surface Charge on Gravitational- Wave Detector Optics

**Honors Thesis
Trinity University Physics Department
Spring 2007**

**Robert McKinney
Advisor: Dr. Dennis Ugolini**

Table of Contents

Abstract	3
Chapter 1: Background Information	4
Section 1.1: LIGO	4
Section 1.2: Charging	6
Section 1.3: Previous work and our goal	11
Chapter 2: Capacitive Probe	14
Section 2.1: Kelvin probe method	14
Section 2.2: Our capacitive probe	15
Chapter 3: Probe Characterization in Air	22
Section 3.1: Verifying the chopper concept	22
Section 3.2: Calibrating the probe	23
Section 3.3: Problems in air	24
Chapter 4: Probe Characterization in Vacuum	29
Section 4.1: The vacuum system	29
Section 4.2: Problems encountered	29
Section 4.3: Measured data	29
Section 4.4: Future improvements and goals	30
Conclusions	35
Sources	36

Abstract

The accumulation and fluctuation of surface charge on the highly reflective optics in the Laser Interferometric Gravitational-Wave Observatory (LIGO) has been determined to be a potential source of noise in the detection of gravitational waves. To test this, a capacitive probe was built using a tuning-fork optical chopper with grounded blades to modulate the capacitance. This probe was used to measure the amount of surface charge and the time it takes for that surface charge to decay on a fused-silica optical substrate in a vacuum environment of 10^{-5} torr. The probe was determined to have a sensitivity of $(2.3 \pm 0.3) \cdot 10^5 \text{ e}^-/\text{cm}^2$. Charges on the order of $8 \cdot 10^7 \text{ e}^-/\text{cm}^2$ and a discharge time constant on the order 170 days was measured for the optic.

1 Background Information

1.1 Laser Interferometric Gravitational-Wave Observatory

Einstein's General Theory of Relativity predicts the existence of waves in space known as gravitational waves. A gravitational wave is a quadrupole fluctuation in space-time due to the movement of massive objects in the universe, such as two black holes spiraling into each other. Gravitational waves are still only theoretical because they have yet to be directly detected. The Laser Interferometric Gravitational-Wave Observatory (LIGO) was created to directly detect fluctuations in the curvature of space due to gravitational waves (see Figure 1). LIGO's secondary goal is to open a new window on the universe and do gravitational wave astrophysics. Some of the more exciting possibilities include: obtaining unequivocal evidence for the existence of black holes; determination of the spin of gravity's quantum-mechanical particle, the graviton; inference of the difference in speed between gravitational waves and light, which theory predicts to be zero if the graviton has zero rest mass.¹⁻³

Gravitational waves are experienced as a strain in space, a change in length per unit length, $\Delta l/l$. The reason we do not feel the universe constantly warping around us is that these strains are extremely small on Earth, since there are no large gravitational wave events in our region of the universe. Gravitational waves are quadrupoles, meaning that they change space in directions perpendicular to their direction of motion. So if a gravitational wave is traveling in the z direction, then the x and y directions will change by the same amount, but in opposite directions. So if one stretches, the other shrinks (see Figure 2).

An example of a large gravitational wave event would be the collision of two massive black holes (~ 10 solar masses). The forces involved would be so great that by the time the black holes collided, the frequency of their rotation would be in the audible range. If this were to happen 100 megaparsec (Mpc) away it would produce a strain on Earth between 10^{-20} and 10^{-22} in the frequency range of 10-1000 Hz. That is roughly equivalent to changing the distance from the Earth to the Sun by the width of an atom. Other sources include the coalescence of two neutron stars and asymmetric supernova explosions. An asymmetric type II supernova explosion at 15 Mpc would produce a strain around 10^{-21} in the 100-1000 Hz frequency range. Advanced LIGO will be able to measure farther. As far out as the Virgo cluster, a large cluster of galaxies in the constellation Virgo approximately 20 Mpc away, type II supernova are estimated to occur at a rate of one or more per year within 20 Mpc away in every direction.²

To detect these minute changes in distances, LIGO uses interferometer technology. An interferometer is a device that operates on the principle of light interference. The Michelson interferometer setup has light entering in from one side, hitting a beam splitter and traveling in two directions (Figure 3). Both paths hit mirrors and bounce back into the beam splitter. The recombined light produces an interference pattern which is measured by a photodetector. If the two paths are in phase or an integer number of wavelengths apart, $n \cdot \lambda$, then constructive interference will occur and there will be a bright band at the photodetector. If the two paths are a half of a wavelength apart or an odd integer times $\frac{1}{2}$ wavelength apart, $(n+1/2) \cdot \lambda$, then destructive interference will occur and there will be a dark band at the photodetector. Interferometers are useful

because they can be used to detect very small changes in distance by counting the number of bright or dark bands that pass the photodetector. That number is equivalent to a change in distance of n wavelengths in one of the arms of the interferometer.

LIGO is a Michelson interferometer with an effective arm length on the order of 10^2 km.¹⁻² The arm length of an interferometer is the distance from the beam splitter to the mirror and back, or the distance that the light travels. Each branch of the LIGO interferometer is 4 km long. The arm length is greatly increased by making all of the optics very highly reflective. This ensures that the light will bounce back and forth many times before it finally exits the arm, having effectively traveled hundreds of kilometers. Since LIGO is trying to measure a strain instead of an actual distance change, then lengthening the arms greatly increases the sensitivity. If the effective length were increased to 1000 km (10^6 m), then LIGO has to measure a change in distance of 10^{-15} m to detect a strain of 10^{-21} , which is within detection limits.

Ideally, the only signals that LIGO would detect would be from gravitational waves, but there are several known noise sources that make detection difficult (see Figure 4). These noise sources set the sensitivity limit for gravitational-wave measurements. At lower frequencies (below about 70 Hz), the sensitivity limit is set by seismic noise. The Earth constantly has seismic waves passing through it that cause vibrations at many frequencies (ground vibrations due to the seismic background, to man-made sources such as traffic on roads or railroads, or to wind forces coupled to the ground by trees and buildings).¹⁻² This seismic motion is transmitted through to the optic through its suspension wire. LIGO uses harmonic oscillators (pendulums and springs) to limit the seismic noise. The optic is suspended as a pendulum and set on top of a system of four layers of masses and springs to reduce the effect of this noise. Pendulums and springs have a resonant frequency at which they naturally oscillate. A forced harmonic oscillator or driven pendulum has a large amplitude when driven at its resonant frequency, but at frequencies above its resonant frequency the amplitude of vibration falls off as $1/f^2$.⁵⁻⁶ The resonant frequency of the pendulum and spring system is about 1 Hz. Since there are a total of 5 different oscillators, the $1/f^2$ effect is multiplied five times, $(1/f^2)^5$, giving a fall off rate of $1/f^{10}$, allowing for the steep slope shown on the noise plot¹⁻² (Figure 4). The harmonic oscillators are only designed to protect the optic from small seismic vibrations. Should a suspension cable break or should the optic start to swing violently, earthquake safety stops are in place to catch the optic, limiting the motion to millimeters (Figure 5).

In the intermediate frequency range (70-200 Hz), the dominant noise limit is thermal noise, Brownian motion driven by thermal excitations (Figure 4).¹⁻²

The third dominant known noise source is shot noise from the laser. LIGO uses an infrared laser with a power output on the order of 10 Watts. Lasers are not entirely monochromatic; they produce a range of wavelengths called the linewidth. The graph of number of photons, N , versus wavelength, λ , for any laser is a Gaussian shape with a width that is proportional to the square root of the maximum number of photons, \sqrt{N} . This means that at any time the fractional change in wavelength is proportional to the width of the curve divided by the height of the curve, \sqrt{N}/N or $1/\sqrt{N}$. This is the limit to the amount of phase change that can be detected in the interferometer. The phase change, $\Delta\Phi$, is given by the equation:

$$\Delta\Phi \approx B \frac{\Delta L}{\lambda} = B \frac{hL}{\lambda} \quad (a)$$

where B is the mean number of times the light bounces back and forth inside the cavity, h is the strain $\Delta L/L$, and λ is the light's wavelength. Since $\Delta\Phi$ is equivalent to $1/\sqrt{N}$, the gravitational-wave strain that would be equivalent to this fluctuation (or the minimum strain that could be measured) is:

$$h_{\min} \approx \frac{\lambda}{L} \frac{1}{B} \frac{1}{\sqrt{N}} \quad (b)$$

This relation ($h_{\min} \sim 1/B$) only works if the mean light storage time in the cavities, BL/c , is less than half of a gravitational-wave period. If B is made larger, there is no improvement. So with 4 km arms and a frequency of 100 Hz, the limit is $B \approx 400$.¹ As frequency increases, then wavelength would decrease, and by Equation (a) the phase fluctuation would then increase, which increases the amount of noise. So above about 200 Hz, shot noise increases with frequency as shown in Figure 4.

Shot noise is also the reason for the orientation of LIGO's arms. In an interferometer, the difference in length between the two arms determines the interference pattern at the end. LIGO's arms are set for destructive interference (interference patterns are shown in Figure 6). If the interferometer was set for constructive interference, then there would always be at least some light at the photodetector, and with that light there would always be shot noise in the signal. It is much easier to set it for destructive interference because no light corresponds to no shot noise.

Another known source of noise is air. Air is harmful to the experiment for several reasons. Air molecules carry a small amount kinetic energy and momentum. This momentum is transferred to the optic whenever a molecule collides with it, creating a false signal. Air also has a slightly larger index of refraction than vacuum, meaning that light travels slower in air. This would not be a problem if the air was uniform, but over the long distance that light has to travel in LIGO, there would be pressure pockets or places where there is more or less air than other areas. Light would speed up or slow down as it passes through one of these pockets, so the time it takes light to travel down each arm would be different. Some light is also lost due to scattering off of air molecules, which decreases the power inside the arm. Finally, air carries with it hydrocarbons that can adhere to the optic, increasing its absorption. Increased absorption decreases reflectivity, thereby shortening the effective arm length and decreasing the sensitivity of the interferometer. To correct for all these potential hazards, LIGO is placed in the largest vacuum system in the world, kept at a pressure of 10^{-9} torr. Since atmosphere is well accounted for, it is shown as a very small contributor to the noise curve in Figure 4.

1.2 Charging

The buildup and fluctuation of excess charge on the surface of the optic is also a possible source of noise. Charging of the optic can occur from several different sources. One is due to dust that is moved during the pumpdown of the vacuum system. If dust collides with the optic while air is being pumped out, it can impart small amounts of

surface charge due to friction. Charge may also be deposited by collision with the earthquake stops (Figure 5). When the optic runs into one of these stops, the contact between the two will leave some amount of surface charge on the optic. As a third source of charge buildup, whenever the optic is exposed to the air or cleaned there is always the chance of surface charge being imparted.⁷⁻⁸

Another possible source of surface charge buildup is due to cosmic ray muons colliding with the beam tube and creating a shower of charge that collides with the optic. In a LIGO Science Collaboration (LSC) internal note from 1996, R. Weiss says that the buildup of surface charge due to cosmic rays would be negligible.⁷ More recently, V.B. Braginsky of Moscow State University did a theoretical study of electric charge buildup that would be imparted on an optic over time due to cosmic rays. Braginsky says that over a period of several months occasionally there will be a large jump in charge attributed to a cosmic ray. The observed fluctuation given is a change in surface charge density of $d\sigma/dt \approx 10^5 \text{ e}^-/\text{cm}^2$ per month, with jumps of up to $10^8 \text{ e}^-/\text{cm}^2$ possibly due to high energy cosmic ray electron scattering.⁹

To see the effects of charging, first consider what happens if the charge is static. If the optics are perfect insulators, then any charge that is imparted will not move around on the surface. Static charge can cause two problems. The first is that it is a threat to the reflectivity of the optics since charge is known to attract dust. Even at vacuum, some dust still remains. Any stray particles will adhere to the stray charge on the optic and will interfere with the reflectivity. Since reflectivity is crucial to achieve the effective arm length, this can decrease the total sensitivity of LIGO. The second problem that static charge can cause is that it can create an electric attraction between the optic and any conductors in the area. This could create problems by either causing the optic to move or causing difficulties in steering and aligning the optic.

However, the optic is not a perfect insulator; therefore, the charge is going to redistribute to some extent. Fluctuating charge would cause fluctuations in electric and magnetic forces that could interfere with the positioning magnets. Fluctuations in electric force could over time cause vibration of the whole optic with respect to conductors in the vacuum tube, such as the suspension frame.

The fluctuation of surface charge can be described as a Markov process. A Markov process is a process in which whatever state, P_n , the system is in at any given moment, that state depends only on the previous state, P_{n-1} . The correlation time, τ_0 , is the time it takes for the system to go from one state to another.¹⁰ For charge fluctuations on an insulating surface, τ_0 can be assumed to be very large since charge does not move easily on an insulator.

This derivation can be found Landau and Lifshitz's Statistical Physics.¹¹ Let $F(t)$ denote the difference between the actual value of the fluctuating force and the average value. Between the values of $F(t)$ at different times there exists some correlation, so that $F(t)$ affects the probabilities of different values at time $t+\tau$. The time correlation can be specified by the mean values of the product $F(t)F(t+\tau)$. This product, ϕ , can be represented as:

$$\phi(\tau) = \overline{F(t)F(t+\tau)} \quad (c)$$

The Fourier transform of $F(t)$ is defined thus:

$$F_{\omega} = \frac{1}{2\pi} \int_{-\infty}^{\infty} F(t) e^{i\omega t} dt \quad (d)$$

Then the inverse of this transform is:

$$F(t) = \int_{-\infty}^{\infty} F_{\omega} e^{-i\omega t} d\omega \quad (e)$$

We can also define a future time, $t' = t + \tau$, so that (c) now becomes:

$$\phi(\tau) = \phi(t' - t) = \overline{F(t)F(t')} \quad (f)$$

Inserting (e) into (f) for each F , we obtain:

$$\phi(t' - t) = \int_{-\infty}^{\infty} \int_{-\infty}^{\infty} \overline{F_{\omega} F_{\omega'}} e^{i(\omega t + \omega' t')} d\omega d\omega' \quad (g)$$

What we have now is ϕ as a function of t and t' , but what we want is ϕ as a function of τ . To do this we have to make ω' a multiple of ω . If ω' is set equal to $-\omega$, then we can write the integrand as having a delta function $\delta(\omega + \omega')$:

$$\overline{F_{\omega} F_{\omega'}} = (F^2)_{\omega} \delta(\omega + \omega') \quad (h)$$

Inserting this into (g) yields:

$$\phi(t' - t) = \int_{-\infty}^{\infty} \int_{-\infty}^{\infty} (F^2)_{\omega} \delta(\omega + \omega') e^{i(\omega t + \omega' t')} d\omega d\omega' \quad (i)$$

Then when we integrate ω' over all space, the delta function becomes a 1 and ω' is now equal to $-\omega$. This makes the exponential, $e^{i(\omega t + \omega' t')}$ equal to $e^{i\omega(t - t')}$. Now ϕ is a function of τ .

$$\phi(\tau) = \int_{-\infty}^{\infty} (F^2)_{\omega} e^{-i\omega\tau} d\omega \quad (j)$$

The inverse of this transform is then:

$$(F^2)_{\omega} = \frac{1}{2\pi} \int_{-\infty}^{\infty} \phi(\tau) e^{i\omega\tau} d\tau \quad (k)$$

Let $F(t)$ have, at some moment t , a value which is large compared with the mean fluctuation. Immediately after this moment, $F(t)$ will tend to return to the equilibrium state. Owing to this assumption, the rate of change of $F(t)$ will be completely dependent

on F itself: $F' = F'(F)$. If F is still compared to the range of possible values, then $F'(F)$ can be expanded in powers of F ; keeping only the linear term:

$$\frac{dF}{dt} = -\lambda F \quad (l)$$

where λ is a positive constant with units of inverse time.

Now we introduce a new quantity, $\xi_F(\tau)$, which we will define as the mean value of $F(t)$ at time $t + \tau$. Using $\xi_F(\tau)$, equation (f) can be rewritten as:

$$\phi(\tau) = \overline{F \xi_F(\tau)} \quad (m)$$

The averaging is now carried out only over the probabilities of different values of F at the initial time t .

Now as in (l), for ξ_F large compared to the mean fluctuation, we have that:

$$\frac{d\xi_F(\tau)}{d\tau} = -\lambda \xi_F(\tau) \quad (n)$$

As defined, $\xi_F(0) = F$, so that when (n) is integrated we get:

$$\xi_F(\tau) = F e^{-\lambda\tau} \quad (o)$$

Substituting this into (m):

$$\phi(\tau) = \overline{F \cdot F} e^{-\lambda\tau} = \overline{F^2} e^{-\lambda\tau} \quad (p)$$

Now if we go back to equation (k) and plug in the new value of $\phi(\tau)$:

$$(F^2)_\omega = \frac{1}{2\pi} \int_{-\infty}^{\infty} \overline{F^2} e^{-\lambda\tau} e^{i\omega\tau} d\tau \quad (q)$$

Integrating this gives:

$$(F^2)_\omega = \frac{\lambda}{\pi(\omega^2 + \lambda^2)} \overline{F^2} \quad (r)$$

λ can be defined as $1/\tau_0$, where τ_0 is a correlation time constant, since λ is an inverse time; see equation (o). Also $\omega = 2\pi f$. Using these, (r) becomes:

$$(F^2)_\omega = \frac{\overline{F^2}}{\pi\tau_0 \left(\frac{1}{\tau_0^2} + (2\pi f)^2 \right)} \quad (s)$$

If we assume that τ_0 is very large with respect to LIGO's sensitive frequency band (bigger than a second), then the $(1/\tau_0)^2$ term is insignificant. In this case, equation (s) simplifies to:

$$(F^2)_\omega \approx \frac{\overline{F^2}}{\pi\tau_0(2\pi f)^2} \quad (t)$$

This equation helps describe the fluctuations of the electric force. It is known as the fluctuating force power spectrum. The fluctuating force depends upon the average force value, the frequency of the fluctuation, and the correlation time between states. If the correlation time of the system is large, then the fluctuations are small. For a conducting surface, the correlation time would be very small and the fluctuations would be large.

From equation (s), if we were to take the square root and then take two time integrals (divide by angular frequency squared) and divide by mass, then Newton's 2nd Law yields an equation for displacement in terms of average force over all frequencies, the time constant, and also frequency.

$$\frac{\sqrt{(F^2)_\omega}}{m\omega^2} = x \quad (u)$$

This new equation would look like this:

$$x = \frac{1}{m(2\pi f)^2} \sqrt{\frac{\overline{F^2}}{\pi\tau_0\left(\frac{1}{\tau_0^2} + (2\pi f)^2\right)}} \quad (v)$$

The important thing to note from this equation is that depending on the size of τ_0 , x (displacement of charge) will depend on a different power of frequency. If τ_0 is large, the $1/\tau_0^2$ term drops out and x depends more on $1/f^3$; but if τ_0 is small, the $1/\tau_0^2$ is significant and x depends more on $1/f^2$. This is significant because there is a possibility that this was observed in October 2006 (see Figure 7). As is shown in the data gathered on October 17, 2006 from the LIGO Hanford facility, there is a bend in the sensitivity measurement (dark black portion) at 1000 Hz. At frequencies below the bend, the slope fits a $(1/f)^2$ relationship, but above the bend, the slope fits a $(1/f)^3$ relationship. This would suggest that at the bend, $1/\tau_0^2$ is equal to $(2\pi f)^2$. This would correspond to a time constant τ_0 of roughly 1 ms, which is much lower than anything previously predicted.

This noise fluctuation is why it is important to devise a way to measure charging of LIGO optics and its effects. A τ_0 of 1 ms would mean that any amount of charge on the optic will fluctuate rapidly, causing false signals. The two unknowns that need to be measured for this charging problem are the amount of charge, q , and the correlation time, τ_0 .

1.3 Previous work and our goal

The goal of our experiment is to design and implement a method of measuring the amount of charge that can buildup on optic material from collisions with earthquake stops and conductors, the fluctuation of that charge in vacuum, and the correlation time of the optic in vacuum. Other studies have shown possible thermal noise effects from charging, although at much higher charge levels than expected or different geometries from current interferometers¹². To measure the quantities in question, we have designed and built a capacitive probe with a sensitivity goal of measuring a fluctuation on the order of 10^5 e⁻/cm², the measured monthly fluctuation of a fused silica optic by Moscow State University¹⁴. If charging is proved to be a significant noise source, then a proposed remedy for optic charging comes from the LISA project.^{8,13} Charge can be directly removed from the optic through illumination with UV light. Before this can be put into practice though, a means of measuring the contact potential of the optic has to be devised; otherwise, there is no way of knowing how much UV light to apply to the optic.



Figure 1: LIGO Site in Hanford, WA

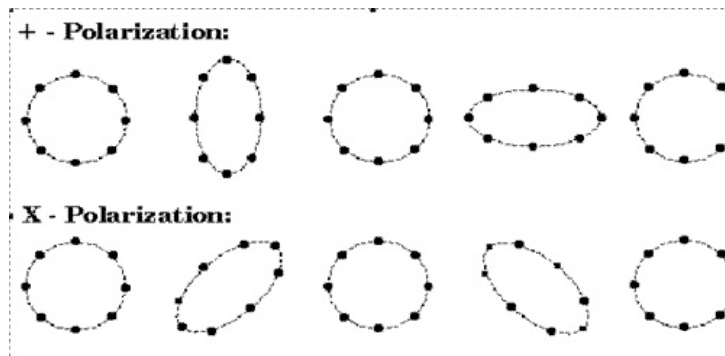


Figure 2: Quadrupole Polarization

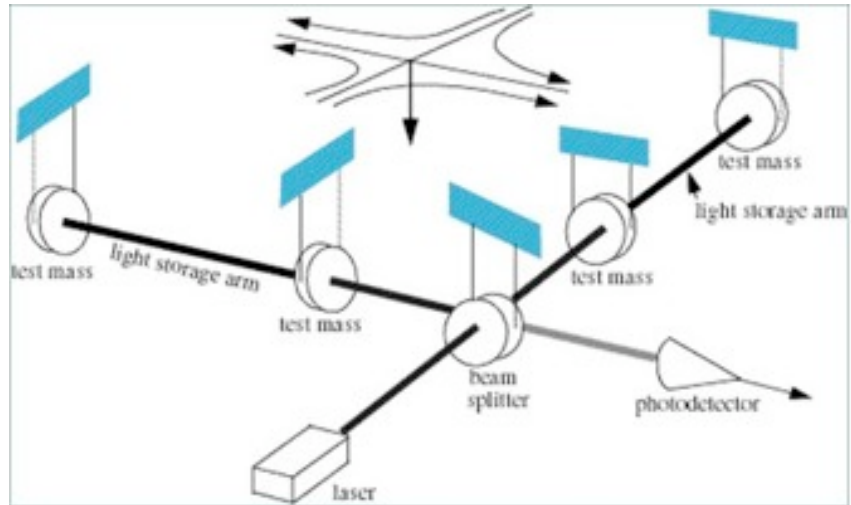


Figure 3: LIGO Interferometer Setup

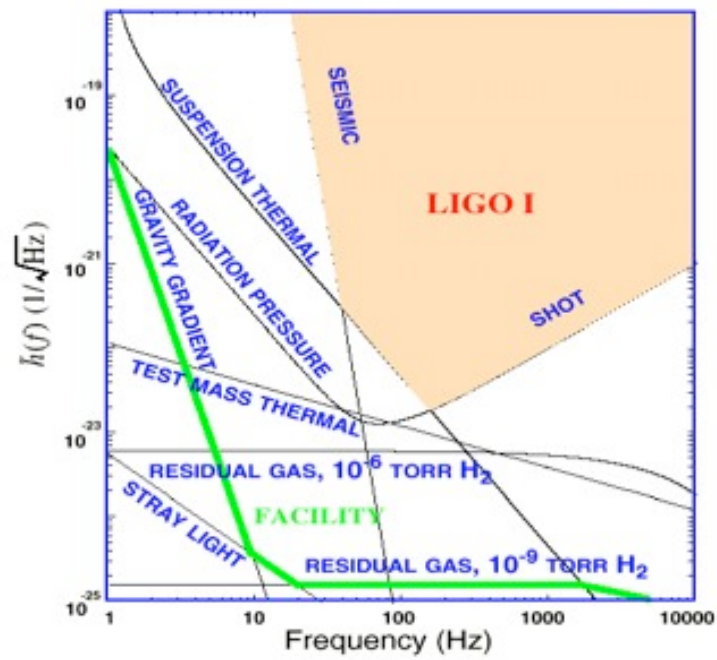


Figure 4: LIGO Noise Plot

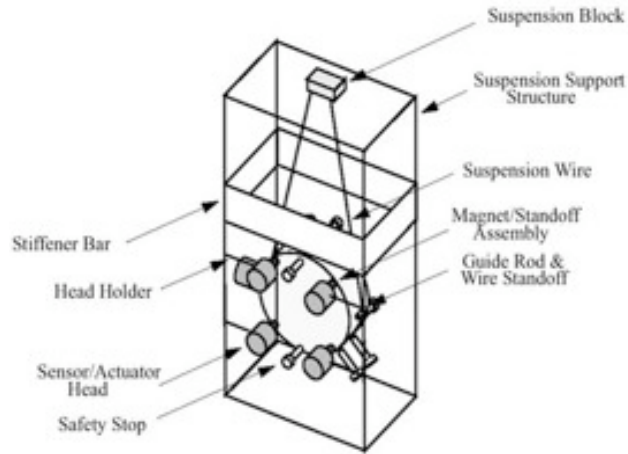


Figure 5: Optical Pendulum

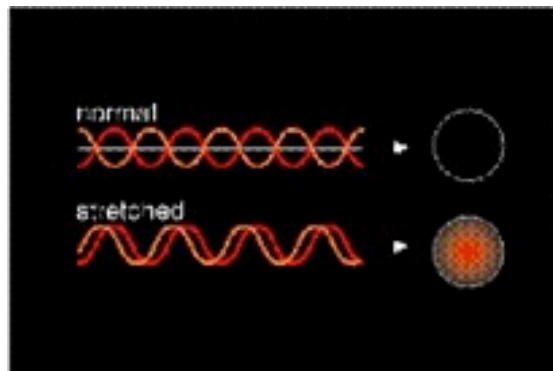


Figure 6: Interference Pattern (top – normal; bottom - stretched)

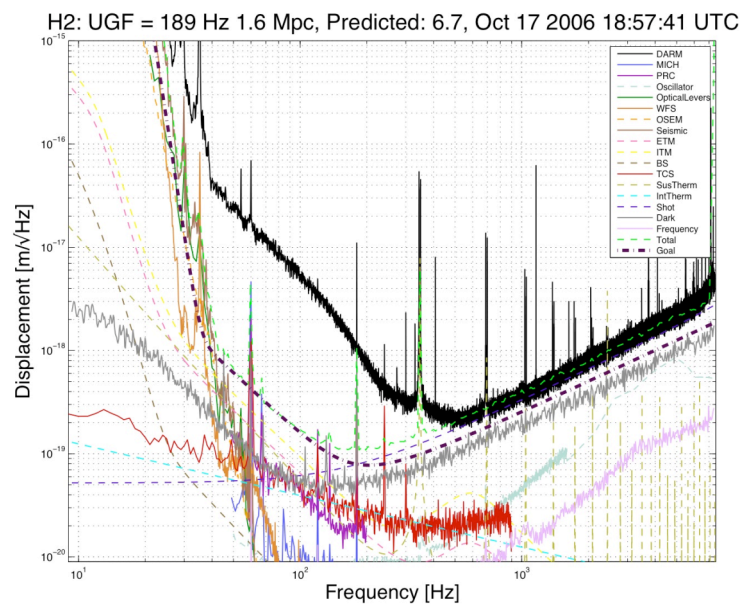


Figure 7: LIGO Noise Data (10-17-2006)

2 Capacitive Probe

2.1 Kelvin probe method

The capacitive probe that we have built is based on the Kelvin Probe method. This method was first developed by Scottish physicist Sir William Thompson (later Lord Kelvin) in 1898.¹⁵ When two conductors are brought into electrical contact a potential difference is generated between the surfaces. This contact potential difference depends on the work functions of the materials being used. The work function is the amount of energy needed to remove electrons from a material's surface, and is related to the material's optical, electrical, and mechanical properties. When two materials with different work functions are brought together, electrons in the material with the lower work function flow to the one with the higher work function. If these materials are separated and made into a parallel plate capacitor, equal and opposite surface charges form on them. The voltage developed over this capacitor is called the contact potential difference. This potential difference is measured by applying an external potential to the capacitor until the surface charge disappears; at that point the applied potential difference will equal the contact potential difference.¹⁵

The Kelvin probe is a capacitive device. A contact potential difference on a conducting sample will cause charge to flow to the surface of the conducting tip of the probe. In a Kelvin probe, the sample and the probe element are connected through a large resistance in order for the flow of charge between surface and probe to generate a voltage. By modulating the capacitance of the probe-sample capacitor, the changing voltage across the resistor produces a proportional AC signal.¹² Figure 8 shows a typical Kelvin probe setup. In this setup, the tip of the probe is vibrated above the sample by a voice coil actuator to change the distance between the tip and the sample. This modulates the capacitance of the probe-sample capacitor since the capacitance of a capacitor is inversely proportional to the distance between the two parallel plates:

$$C = \frac{\kappa\epsilon_0 A}{d} \quad (w)$$

In this equation, A is the surface area of the plates, d is the distance between the plates, κ is the dielectric constant of the material between the plates (vacuum would have dielectric constant of 1), and ϵ_0 is a universal constant, the permittivity of free-space. In commercial Kelvin probes, the probe tip is vibrated, which changes the distance in the capacitor.^{12,14} A PZT is a piezo-electric material that expands or contracts depending upon the voltage difference across the crystal, so it makes for a very accurate linear oscillator. A voice-coil is a magnetically driven linear oscillator, the kind of oscillator used to vibrate speakers. Both of these actuators are used to vibrate the probe tip. Figure 9 shows an example of an ultra high vacuum (UHV) compatible head stage using a voice coil driver.¹³

For our research purposes, typical Kelvin probes made with vibrational actuating devices that modulate the distance between probe tip and sample were undesirable because of several restrictions on what our probe had to accomplish. Our intent has been to measure the surface charge on LIGO optics, which are made of fused silica, an

insulating material. We could not, therefore, connect a large resistance between the sample and the tip. Most commercial probes (specifically their readout electronics) are designed with conducting samples in mind. The required sensitivity of our probe was determined by a study at Moscow State that measured the charge drift on fused silica to be $10^5 \text{ e}^-/\text{cm}^2$ per month.¹⁴ This is well within the stated sensitivity of many commercial probes, but it was not a guarantee that the commercial probes would maintain that level of sensitivity when used to measure the surface charge buildup on an insulator. Our probe also had to be vacuum compatible so that it could potentially be placed into LIGO to measure the amount of charge on a working optic. Commercial probes are designed to be used in high vacuum environments; however, one constraint on our probe was cost. We had to design a probe that would operate within our budget. Commercial probes which use PZT or voice coil actuators were outside of our budget; quotes from Besocke Delta Phi GmbH and <http://www.kelvinprobe.com> ranged from \$7,100 - \$12,000 for a vacuum-compatible probe.⁸

2.2 Our capacitive probe

Trying to remain within budget and still modulate the capacitance of the sample-tip capacitor, we took a different approach. Since the cost to modulate the distance between the tip and the sample would be prohibitive, we devised a method of modulating the electric field formed between the tip and the sample. Rai Weiss from LIGO came up with the idea of modulating the capacitance by inserting a tuning-fork optical chopper with grounded blades between the sample and the probe tip. The chopper operates like a pair of scissors, opening and closing at a given frequency, which alternately occludes and exposes the probe tip to the sample. When the blades are open there is an electric field between the tip and the sample, forming a capacitor. When the blades close the probe is shielded from the sample and the tip to probe capacitance goes to zero. The probe capacitance thus alternates between maximum and zero. The CH-10 optical chopper from Boston Electronics Corporation was chosen for its small size, vacuum compatibility, and low cost (~\$850 with driver circuit). The wire coil at the center generates a magnetic field that vibrates the blades at 504.5 Hz.¹² A schematic of the tuning-fork chopper is shown in Figure 10.

Apart from determining whether or not chopper modulation was a feasible method of capacitance modulation, we also had to construct our probe with a conducting tip that would be able to measure the fluctuation desired. This process has led to several versions of probe design, accounting for several design requirements:

- Orientation to sample and chopper* - The probe had to sit above the chopper without touching it, but still be able to be secured to the optical table.
- Proximity to sample* - The signal received from the probe tip was much stronger the closer it was to the sample. The probe setup is shown in figure 11.
- Material and machining cost* - We needed an inexpensive method to machine the probe, which required a simple design made from easily obtained materials.
- Vacuum compatibility* - Eventually the probe needed to be able to work in a high vacuum.

Taking these things into account, our first versions of the capacitive probe were made to be used in air to test if the chopper modulation would work. Our initial design was a long shaft (~ 15 cm long) made from acrylic. This shaft could be attached to an optical post and secured to the optics table. The tip was a small piece of copper (roughly 4 mm^3) soldered onto a wire from which we measured a signal. Surrounding the tip was a large grounded ring of copper used to prevent external electric fields from interfering with any measurement. This initial design is shown in Figure 12.

This first design was undesirable because it was too large. We could only fit the probe within a few centimeters of the sample. Looking at Figure 11 the initial probe was too big and it would hit the magnetic coil on the chopper (located just behind the blades) if we tried to move it too close because the probe extended beyond the tip in the first version. To correct for this we initially tried to sacrifice the grounding ring and make the neck of the probe much smaller. This second generation is shown in Figure 12. While we were able to fit this version of the probe within a centimeter of the sample, we discovered that the grounding ring could not be lost because the background electric fields present were too large to allow for any useful measurement. The noise peak was on the order of several mV even when the sample was removed entirely, which was much larger than the signal we were trying to measure, so no measurement could be made using this probe.

Taking this all into account, we designed a new probe. For a probe we used just a bare wire. This allowed us to make the grounding ring small enough to be able to fit the probe within the desired proximity of the sample. This is the final design shown in Figure 12. One other modification we made to the system at this point was to encase the chopper inside a grounded aluminum box, only allowing the blades to protrude from the box. This greatly reduced any electric fields emanating from the magnetic coil on the chopper body as a noise source. With all of this, we still had a noise peak of 0.1 mV at our 504.5 Hz frequency, which was still large compared to our signal.

However, when using our tuning-fork chopper, we found that we could also detect a signal at 1009 Hz (twice the chopping frequency) with no measurable noise peak and a signal fluctuation of $\pm 0.5\text{ }\mu\text{V}$. The reason is that the chopper has a 50% duty cycle. When the blades are “open”, field lines pass between them to the probe tip. When the blades are “closed”, they overlap, allowing field lines to pass around the outer edges of the blades to the probe; see Figure 13. We were able to verify this by using a laser and photodiode setup, shown in Figure 14. The signal that we read on the oscilloscope from the photodiode is shown in Figure 15. We can compare this to the amplified signal that we were able to read off of an in-air probe, shown in Figure 16. While these two signal plots are not identical, it appears as if Figure 16 is the derivative of Figure 15. This is what we should expect, since we are measuring an induced voltage causing charge to flow to and from the probe tip. This voltage is dependent upon the change in the electric field.

While we were able to use this design to measure signals from insulating samples, the sensitivity was low due to the small surface area of the bare wire tip. To correct for this, we modified this design slightly by adding a drop of solder onto the wire tip, increasing the surface area of the probe. This increased the maximum capacitance of the probe-sample capacitor, since area is directly proportional to capacitance. This allows for a greater AC signal, since the changing voltage will have a greater amplitude. This can be

seen in a calibration graph in Figure 17. The probe without solder has a much smaller tip and thus a lower signal.

With the problems of orientation and proximity solved, the next version of the capacitive probe had to address the issue of vacuum-compatibility. The probe was made out of aluminum and shrunk down to 10 cm long and 1.3 cm wide. The probe was made out of aluminum because it was the easiest vacuum compatible, LIGO-approved material to machine. Plastic of any kind is not allowed because at low pressures plastic outgasses hydrocarbons that pollute optics.¹⁷ The initial versions used copper wire with plastic coating. In this version we used vacuum-compatible Kapton-coated wire. We also used vacuum-compatible silver solder to increase the surface area of the tip. Because the entire probe body was grounded aluminum, an additional grounding ring was unnecessary. The vacuum-compatible probe is shown in Figure 18.

The advantages of our probe are that it has a simple design with the desired sensitivity, is capable of being put into vacuum, and is small enough to be maneuvered into position relative to the chopper and sample. It was very cost effective, since all of the materials are easily obtained and it could be made in our department machine shop. The most expensive part was the chopper itself.

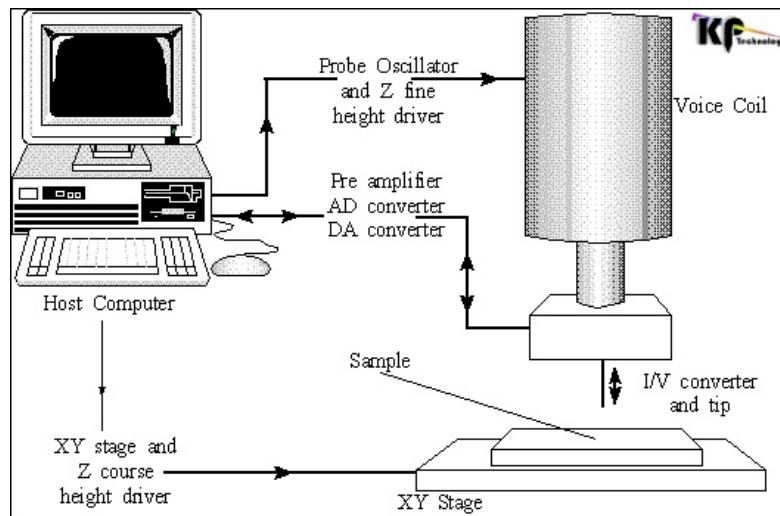


Figure 8: Kelvin probe setup with voice-coil actuator¹⁵



Figure 9: Voice-coil vacuum-compatible actuator¹⁵

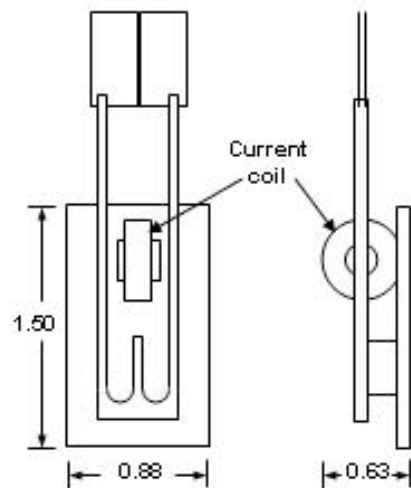


Figure 10: Schematic of tuning-fork chopper

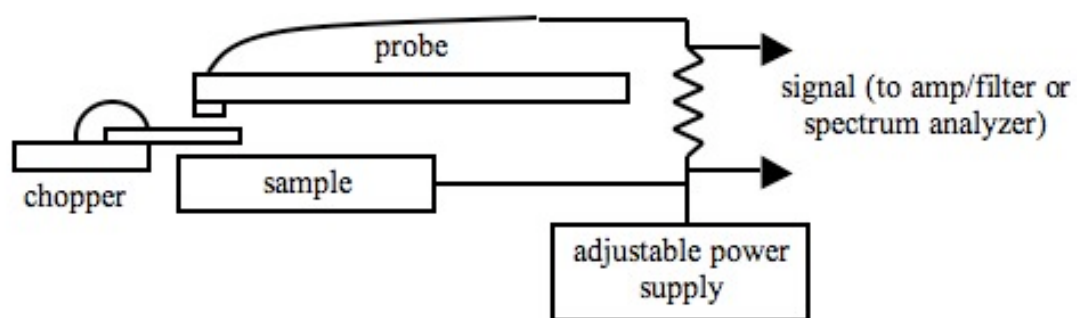


Figure 11: Probe setup with conducting sample and tuning-fork chopper

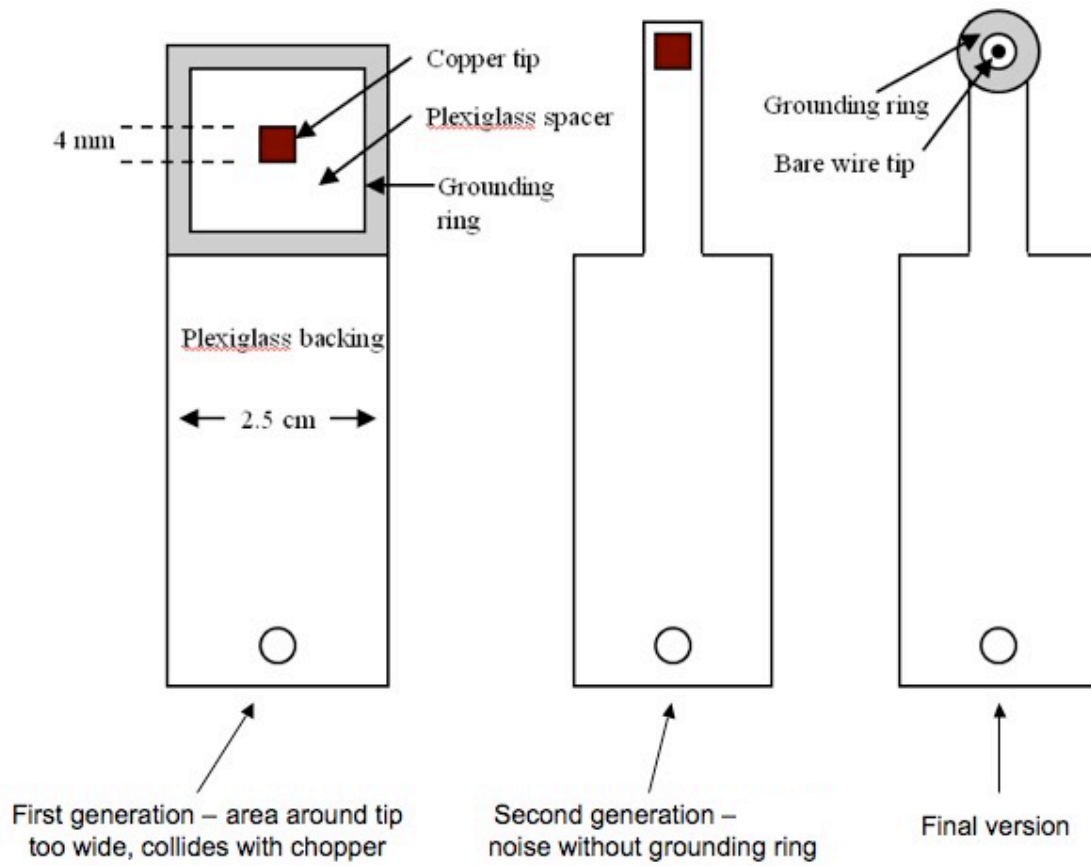


Figure 12: In-air probe designs

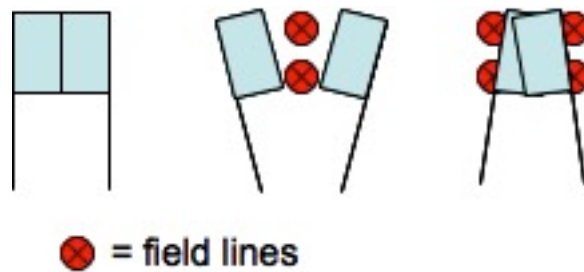


Figure 13: 50% duty cycle on tuning-fork chopper blades

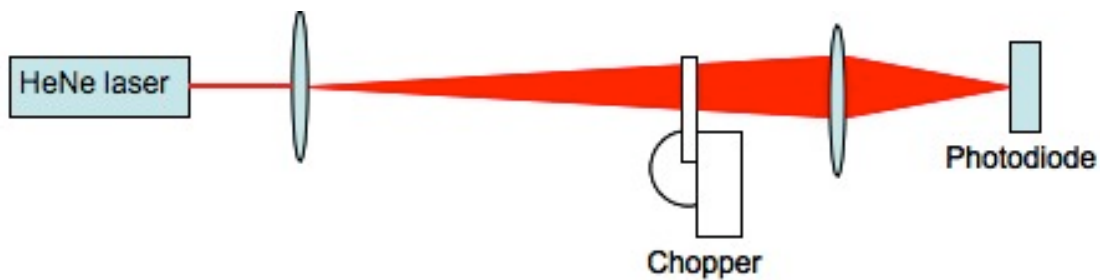


Figure 14: Optical demonstration setup of duty cycle on chopper blades

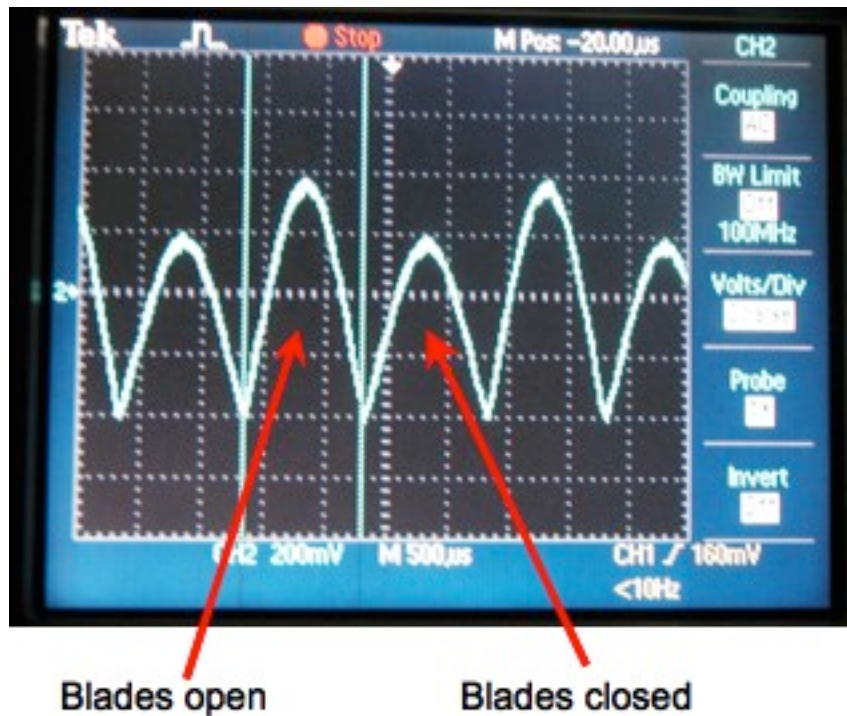


Figure 15: Photodiode signal from optical setup

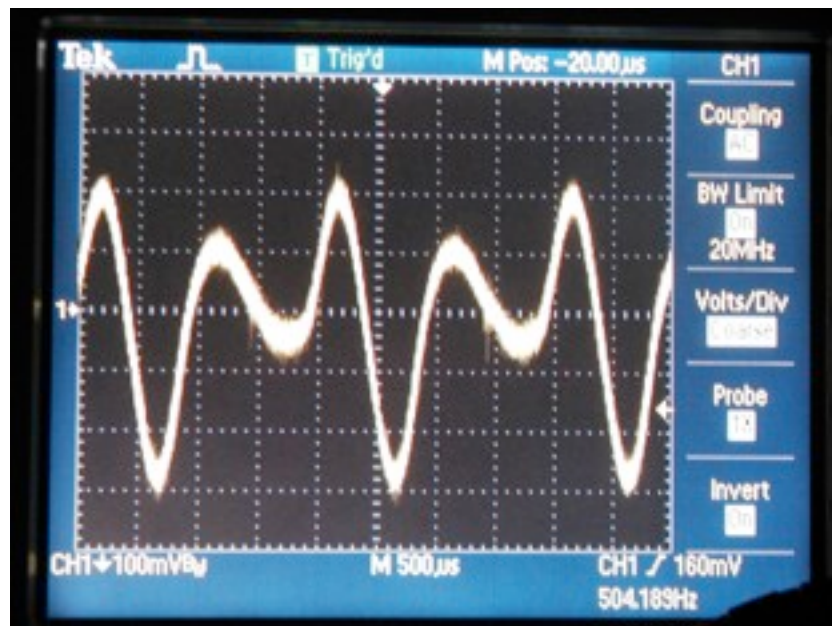


Figure 16: Amplified capacitive probe output with charged insulating sample

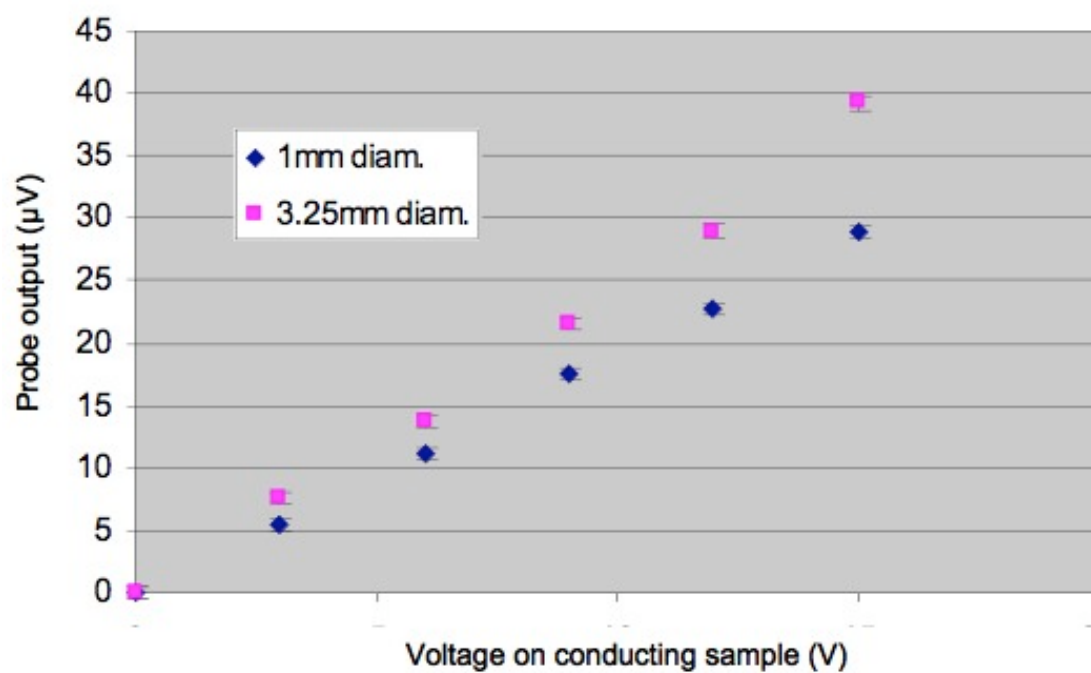


Figure 17: In-air probe both with and without solder tip using rotary chopper and conducting sample (probe to sample distance 6 mm)

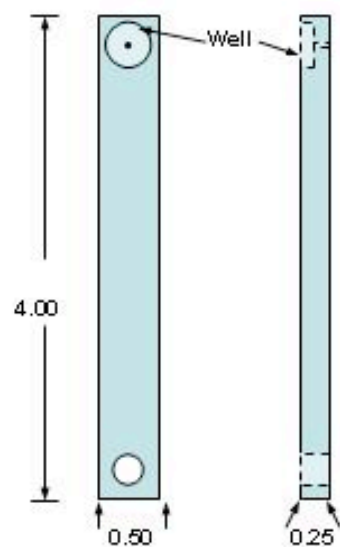


Figure 18: Vacuum-compatible probe

3 Probe Characterization in Air

3.1 Verifying the chopper concept

Once we had our in-air probe in its final form, we were able to determine if the chopper concept was a feasible option for modulating the capacitance of the system. We first tested the chopper concept with a Stanford Research Systems SR540 rotary chopper, which generated less noise at the signal frequency than the tuning-fork chopper and also allowed us to vary the chopping frequency (pictures of both choppers are shown in Figures 19 and 20). We started by using a conducting sample because we could keep the contact potential difference a constant, allowing for consistent results over time. This was more desirable than an insulating sample because any surface charge deposited on an insulating sample would quickly dissipate.

We kept the sample and the chopper stationary and used a micrometer to change the distance between the probe and the sample in the z direction. Using a thin aluminum sample with an applied voltage of 15 volts and tuning the rotary chopper to the same frequency as our tuning-fork chopper, 504.5 Hz, we found that the signal-to-distance relationship was well modeled by an inverse square law. Moving the sample to the side, or just behind, the probe resulted in no signal observed,¹² suggesting that we were measuring a real signal from the sample. Figure 21 shows the response of the probe as a function of distance from the sample. The y-axis represents the probe signal with 15 volts applied to the sample minus the signal with zero volts applied. There is a signal at 0 volts because there is a noise peak that could not be eliminated entirely. Subtracting this gives the actual probe response to distance. Increasing vertical distance between the chopper and sample caused a sharp fall-off in signal, which is why it was so crucial for the probe to be able to be maneuverable close to the chopper and sample.

We also tested the relationship of signal to the horizontal distance between the probe and sample. We kept the sample and the chopper stationary and used a 2-direction micrometer base to move the probe in the x-y plane. Using the tuning-fork chopper and measuring at both 504.5 Hz and 1009 Hz, we were able to record the signal and different x-y coordinates. We mapped out the contour plot shown in Figure 22 for the 1009 Hz signal. The plot has contour lines drawn at every 10% decrease in probe signal. The plot shows that past 1 mm off-center the signal drops by 10%. The 1009 Hz was more desirable for this measurement because there was less noise. The fact that the maximum exists in the center told us that the 1009 Hz signal exists due to the 50% duty cycle and also that we needed to position the probe to within 1 mm of the chopper.

By varying the rotary chopper frequency, we were able to determine that our signal varied at different frequencies. By sweeping through a range of frequencies while keeping the probe-to-sample distance a constant, we obtained the plot shown in Figure 23. We found that the probe had a maximum response around 1 kHz. To model this data we started from the idea of a capacitor. The sample is kept at a constant potential, so when the blades of the chopper are open or overlapped, a capacitor is formed between the sample and the probe tip. The charge on the tip starts at zero and increases in the form of $(1 - e^{-t/RC})$, where R is the impedance of the measuring device (spectrum analyzer) and C is the capacitance of the system (spectrum analyzer plus BNC cables). However, we measure a potential difference that is proportional to the current, the derivative of the

charge, so the function we want is of the form $V = Ae^{-t/RC}$, where A is a constant. We measure a time average of this and since we are measuring at 1009 Hz the time average is only over one half period, $\tau/2$. So then our signal response looks like this:

$$Signal = \frac{1}{\tau/2} \int_0^{\tau/2} V dt = \frac{2}{\tau} \int_0^{\tau/2} Ae^{-t/RC} dt \quad (x)$$

Integrating this yields an equation for our signal:

$$Signal = \frac{2ARC}{\tau} \left[1 - e^{-\tau/2RC} \right] \quad (y)$$

Plugging in frequency, f , for $1/\tau$ making $2ARC$ into a new constant B we can rewrite (y) in terms of signal versus chopping frequency:

$$Signal = Bf \left[1 - e^{-1/2RCf} \right] \quad (z)$$

We were originally using a spectrum analyzer with an input impedance of 1 M Ω and a combined capacitance with BNC cables of 600 pF. This yields a time decay constant of $2RC = 1.2$ ms. This gives a frequency constant around 833 Hz, which makes sense from our graph in Figure 23; above this frequency the signal is almost at a maximum. The probe signal decreases as frequency decreases below this value, reaching zero at DC. Such behavior makes sense -- when the sample is exposed or occluded, a voltage is induced in the probe, causing charge to flow to or from the tip. If the chopping period is too slow, the charge in the tip can reach a steady state, eliminating the induced voltage and our desired signal. From these data we determined that the probe should operate at about 86% of its maximum sensitivity when measuring a signal at 504.5 Hz with our tuning-fork chopper.¹² This is why our discovery of the chopper's 50% duty cycle was so crucial. Measuring at 1009 Hz, we are nearly at the maximum sensitivity of the probe.

3.2 Calibrating the probe

We determined that our probe did work and was able to measure a real surface charge on an insulating sample; however, we needed to find a way to determine how our measurements corresponded to actual surface charge values.

We used a Surface DC Voltmeter to calibrate our probe. The Surface DC Voltmeter is a device that measures potential difference from a surface; see Figure 24. In the manual provided with the voltmeter, we found how to convert a reading on the meter to a measurement of surface charge.¹⁸ According to the manual, a voltage reading on the meter, when reading an insulating surface, is equal to twice the electric field times the distance:

$$V = 2EL \quad (\alpha)$$

The manual also gave an equation for the electric field as a fraction of charge per area, S :

$$E = (5.7 \cdot 10^{10})S \quad (\beta)$$

This equation with electric field in volts per meter for S in Coulombs per square meter. Combining equations (α) and (β) we get:

$$S = \frac{V}{2L(5.7 \cdot 10^{10})} \quad (\gamma)$$

This provides us with a value for the amount of surface charge on the sample in Coulombs per square meter. For our calibration we used a distance between voltmeter and sample of 1 in. (2.56 cm), where the voltage was equal to 5.2 ± 0.7 kV. So using (γ), this gives a surface charge density of $(1.8 \pm 0.2) \cdot 10^{-6}$ C/m² or $(1.1 \pm 0.1) \cdot 10^9$ e⁻/cm².

This is the amount of surface charge on the sample that corresponds to 336 μ V on the probe. When we divide the charge density S by our 336 μ V signal we get the charge density per microvolt on our probe: $(3.3 \pm 0.4) \cdot 10^6$ e⁻/cm²/ μ V. Later on we decreased the separation from 16 mm to 6 mm, so to correct our result we multiply by $(6/16)^2$, giving a new sensitivity of $(4.7 \pm 0.6) \cdot 10^5$ e⁻/cm²/ μ V. Finally, our noise level is ± 0.5 μ V, so the smallest signal visible above the noise is given by: $(2.3 \pm 0.3) \cdot 10^5$ e⁻/cm². This puts the sensitivity of our probe on the initially desired order of magnitude of 10^5 e⁻/cm².

3.3 Problems in air

Once we had the probe calibrated, we tried to charge an insulating sample and measure the decay constant. We found that we could not measure a consistent decay constant for the sample. As shown in Figure 25, the rate of charge decay in air fluctuates from day to day. Our theory was that charge decay in air depends strongly on the amount of moisture in the atmosphere and that it should not be a problem once we moved into the vacuum chamber. On the three days shown we did try to measure the humidity and we found it to be similar for all three; however, we later discovered that our hygrometer was broken. We later obtained a working hygrometer and measured humidity percentage against time decay constant. We found a sharp correlation between humidity and charge decay (see Figure 26). As humidity increased charge dissipated much faster.

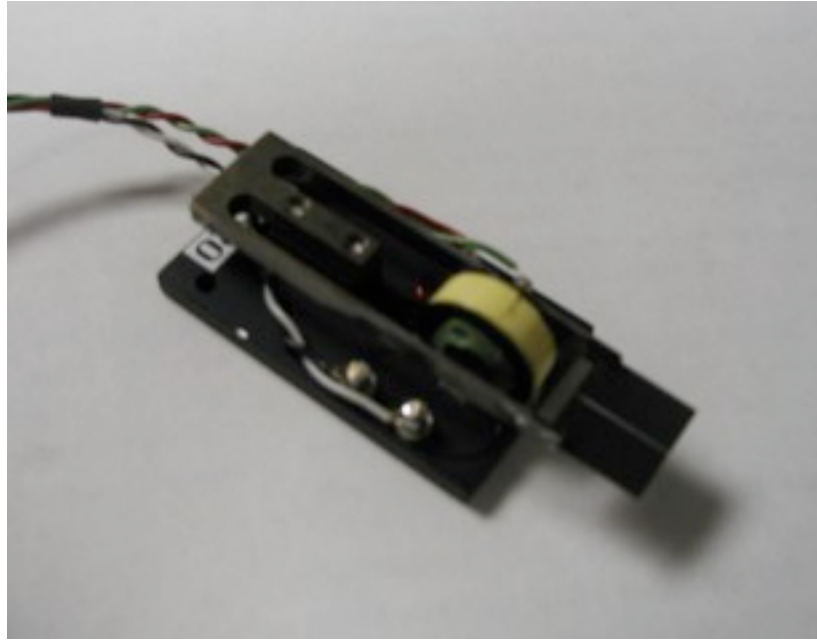


Figure 19: Tuning-fork chopper



Figure 20: Rotary Chopper

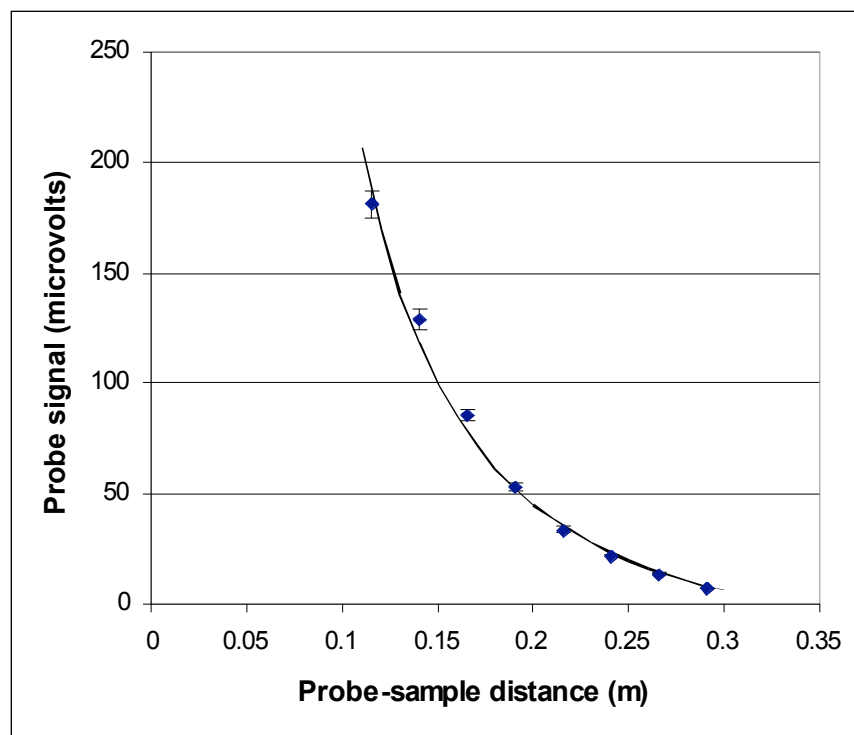


Figure 21: Relationship of probe to sample distance using the rotary chopper

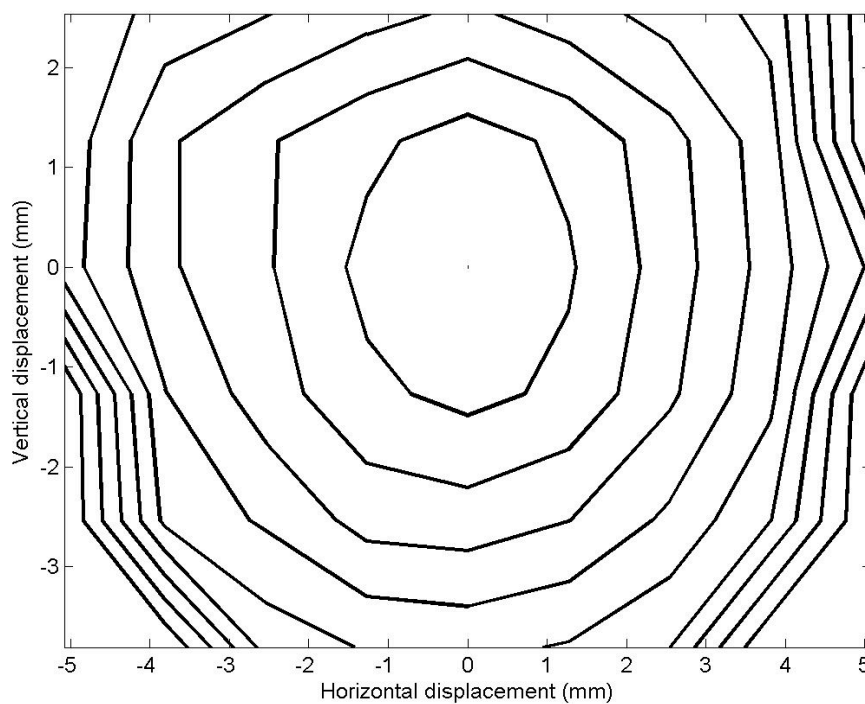


Figure 22: Contour plot of tuning-fork chopper signal at 1009 Hz versus x-y position

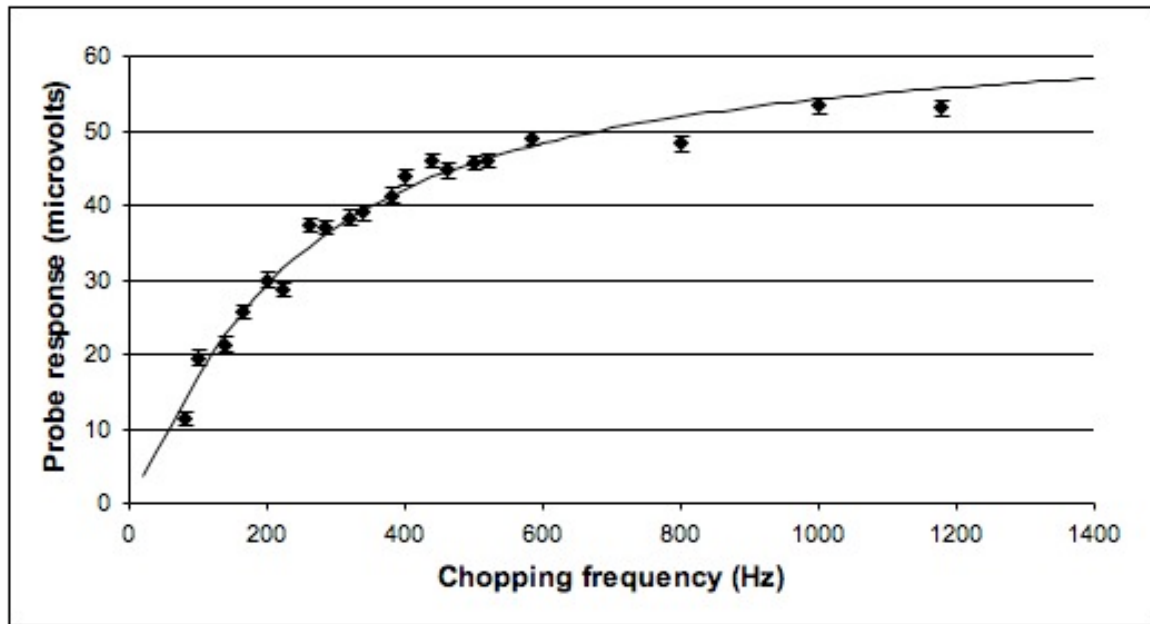


Figure 23: Probe signal versus frequency of modulation



Figure 24: Surface DC Voltmeter

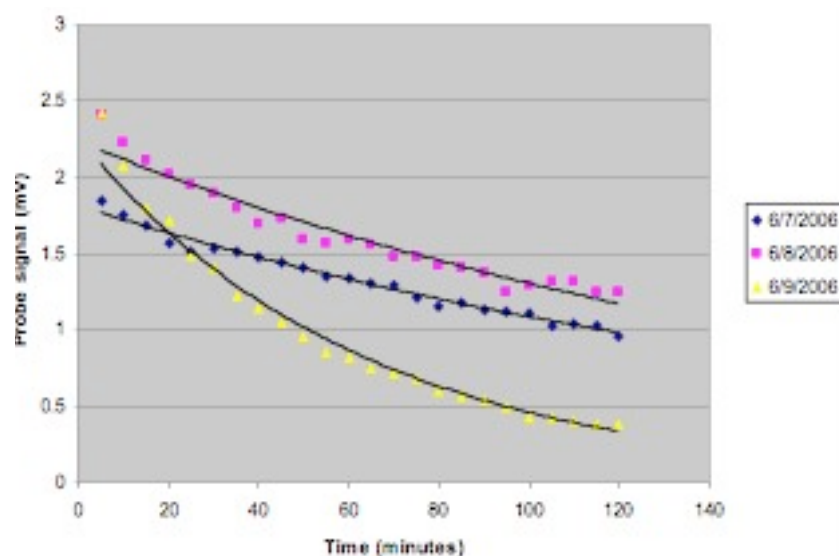


Figure 25: Charge decay over three trials

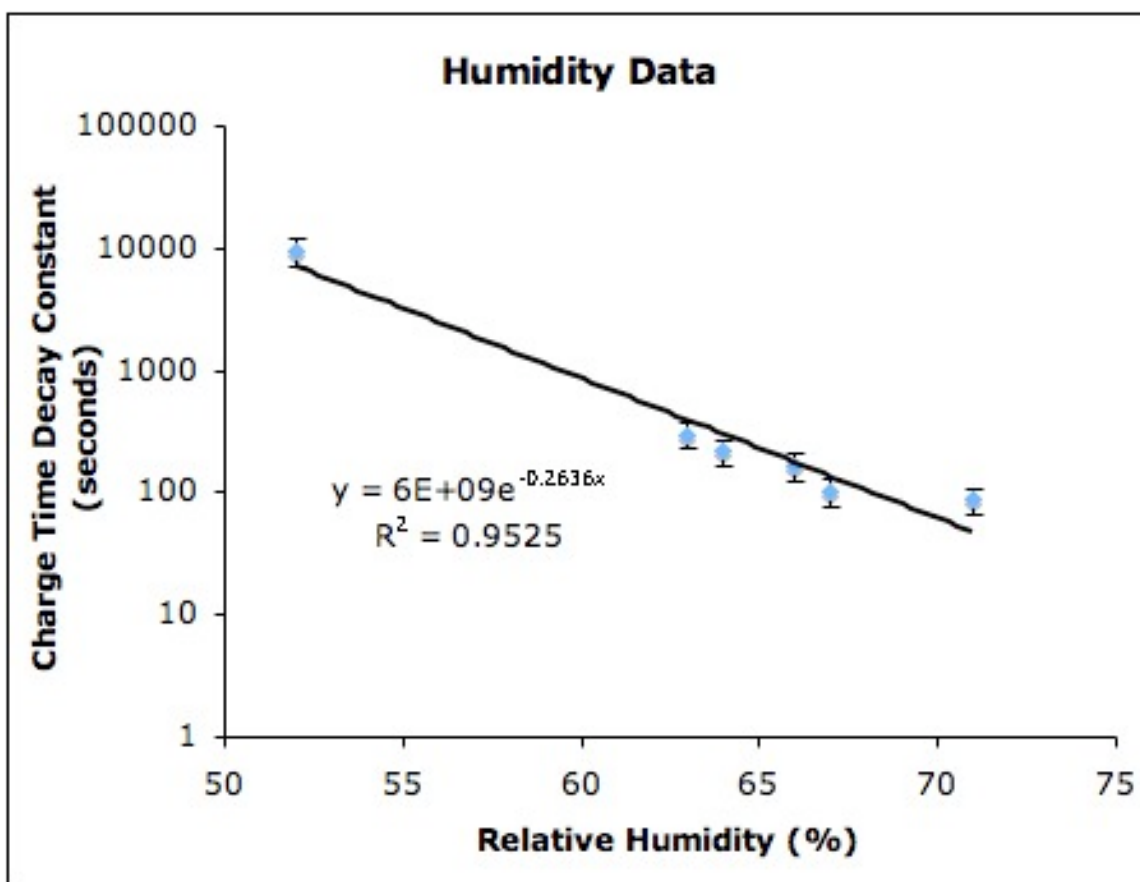


Figure 26: Charge Decay Constant vs. Humidity

4 Probe characterization in vacuum

4.1 Moving the probe into vacuum

Our vacuum system works by having two different types of vacuum pumps. The first is a dry diaphragm vacuum pump that reduces the pressure to around 0.5 torr. After that a turbo-molecular drag pump takes the pressure down to 10^{-5} torr (vacuum system and probe setup shown in Figures 27 and 28). A dry diaphragm pump is basically a bellows that uses no lubricant. A turbo molecular drag pump has a rotor that drags across a membrane and physically knocks the remaining air particles out of the tube. We connected a feedthrough so that we could power the chopper from outside the vacuum and also send the signal to the spectrum analyzer. A feedthrough allows an electrical signal to be passed between vacuum and atmosphere.

4.2 Problems encountered

Upon moving our probe to vacuum, we encountered a problem with the feedthrough. Initially we ran the chopper power supply input and our signal output through the same feedthrough. To pass through the feedthrough the power supply and the signal had to be brought into close proximity. We found that the power supply signal bled over into the probe signal if the wires were close to each other. This caused a dominant noise peak at the chopping frequency. To correct for this, we set up a second feedthrough and ran the power input through one and the signal output through the other. We also tied both wires down to opposite sides of the optical bench to keep them from being loose inside the chamber.

We started by using a spectrum analyzer as our means of measuring the signal produced by surface charge. We found that this was not ideal, since the chopping frequency is not always a constant. We were taking measurements by looking at the peak on the analyzer and recording the height. However, there is a problem of binning, since the spectrum analyzer measures frequencies at intervals (see Figure 29). If the frequency varies, then our peak drops even though the signal may still be the same strength. Because the area of the peak stays the same, a neighboring bin gets bigger as the maximum gets smaller. Evidence for this effect can be seen in Figure 30. We managed to trap a large charge on the optic and get the vacuum system closed and pumped down before the charge could dissipate in the air. However, the signal fluctuated randomly. We believe this was due to the binning effect of the spectrum analyzer. To correct for this we switched to a lock-in amplifier which used the power input of the chopper as a reference, so that the signal we measured at was at the exact chopping frequency. The random oscillations disappeared. The lock-in amplifier also had the benefit of having a $10\text{ M}\Omega$ impedance. As described earlier in Chapter 3, a large impedance on the measuring device provides for a stronger signal at lower frequencies.

4.3 Measured data

After we switched to the lock-in amplifier we measured the decay of surface charge on the optic in vacuum over a time of 16 days. We charged the optic by rubbing it

with a Viton seal, and then we placed it into the vacuum chamber and pumped down to 10^{-5} torr. The signal from this vacuum test was around 200 μV when we placed the optic into vacuum. Using our calibration, this corresponds to a surface charge of $8 \cdot 10^7 \text{ e}^-/\text{cm}^2$ due entirely to friction with the Viton seal. Measuring at 1009 Hz over 16 days we obtained the plot in Figure 31. An exponential fit of this graph yields a time decay constant of 170 days. An interesting thing to note about this is that it appears to level off around day 13; we are not yet certain why. We also recorded the phase difference on the lock-in between the signal and the reference signal from the chopper. For the majority of the data the phase was constant, except for a few points. The points in Figure 31 that lie well below the exponential fit had a large phase change, so we think that there may have been a problem with the lock-in amplifier; on these points the phase would drop by nearly 2 degrees.

We were now able to measure surface charge on a fused-silica optic in vacuum, which was our original intention. Next we tried to discharge the optic. As mentioned briefly at the end of Chapter 1, LISA has experimented with using UV light to discharge the gold-coated optics in their setup. We decided to try this out with our optic. One minor hindrance was that the view port on our vacuum is made out of glass that has only 15% transmission of UV light, so no matter how intense the UV source used, the view port would block 85% of it. First we used a Mercury (Hg) discharge tube. We placed the discharge tube next to the view port of the vacuum tube and left it turned on for several hours. We saw no change in the signal over this time period. We then used a monochromator to determine that the discharge tube was not emitting any UV radiation. This was due to the fact that the glass on the tube was designed to block UV radiation for safety reasons. Next we used a Pen-Ray UV Lamp (253.7 nm, $4.4 \text{ mW}/\text{cm}^2$ at 19 mm) and set it up so that it was shining into the vacuum tube. We obtained the plot shown in Figure 32. The graph gives an exponential fit with a decay constant of 416 minutes. This shows that UV light can be used to discharge the optic much more rapidly than the optic would naturally discharge in vacuum.

4.4 Future improvements and goals

Many things remain to be done with this capacitive probe setup. First, we need a way to charge the optic while it is still in vacuum. When charging the optic in air most of the surface charge is dissipated before the optic can be placed into the vacuum environment. If the optic could be charged while already in vacuum, a much larger signal could be measured and a better decay plot could be achieved. Also, we wouldn't have to open the chamber between each measurement. When charging in air, we were able to get a signal of nearly 1 mV, but by the time we put it into vacuum and pumped down the signal had dropped by a factor of 5 due to charge exchange with air.

Second, a Besocke Kelvin Probe was recently purchased, which uses a PZT driver to vibrate the probe tip. This will be placed into the setup and used along with our chopping capacitive probe to determine if it has a better sensitivity. This will also provide for two probes to be run simultaneously in vacuum. So while one probe is measuring a decay over a long period of time, the other could be used for different experiments.

Third, we need to start measuring the effect of different cleaning methods on the optic and the different reflective coatings. One of the initial reasons for undertaking this

project was that the methods used in cleaning the LIGO optics were known to impart surface charge onto the optic.

Fourth, more testing will be done with UV discharging. Instead of using the glass view port, a quartz view port will be purchased which has a much higher transmission percentage of UV light. Also, a better UV light source can be obtained, one that can be left on for long periods of time. Once this is done a measurement of how long it takes to completely discharge the optic with UV light may be obtained. Also, tests are needed to determine if 254 nm is the best wavelength for discharge.

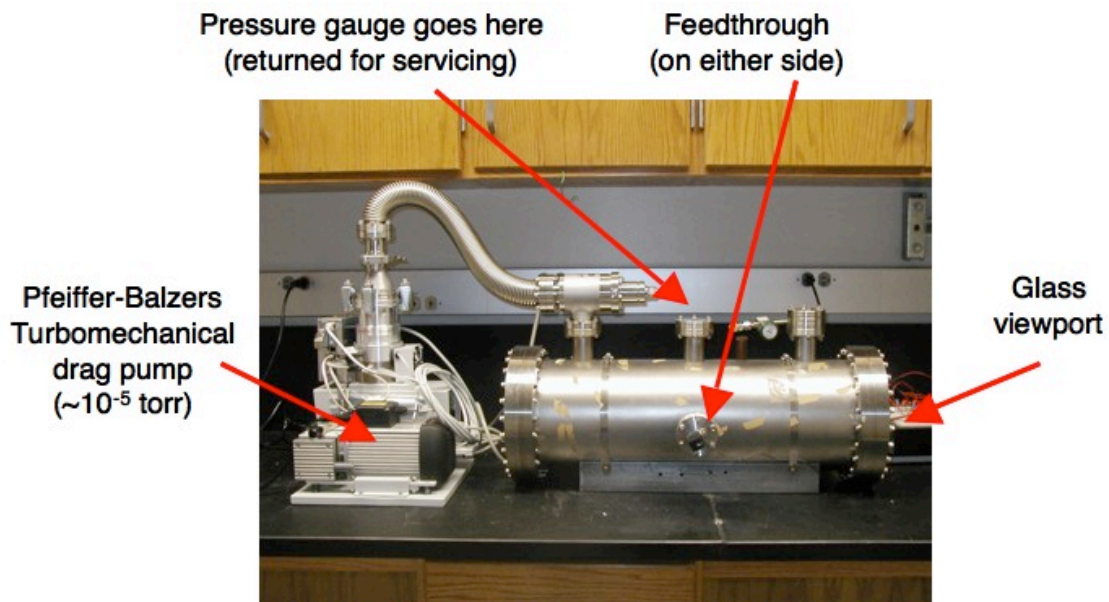


Figure 27: Vacuum system with turbo pump

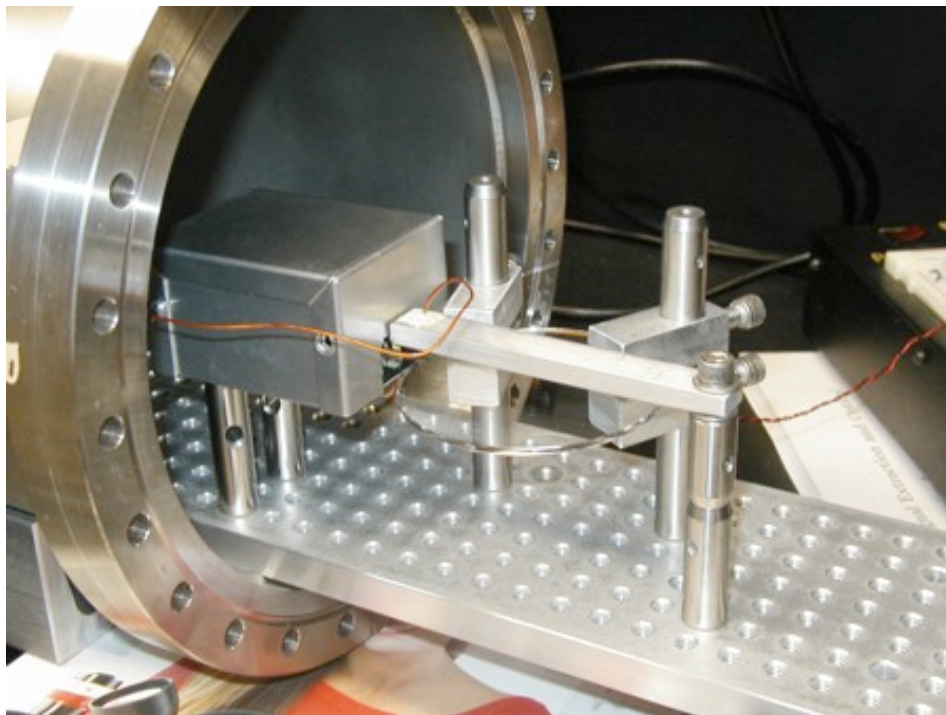


Figure 28: Vacuum setup with aluminum probe, tuning-fork chopper, and fused silica LIGO optic sample

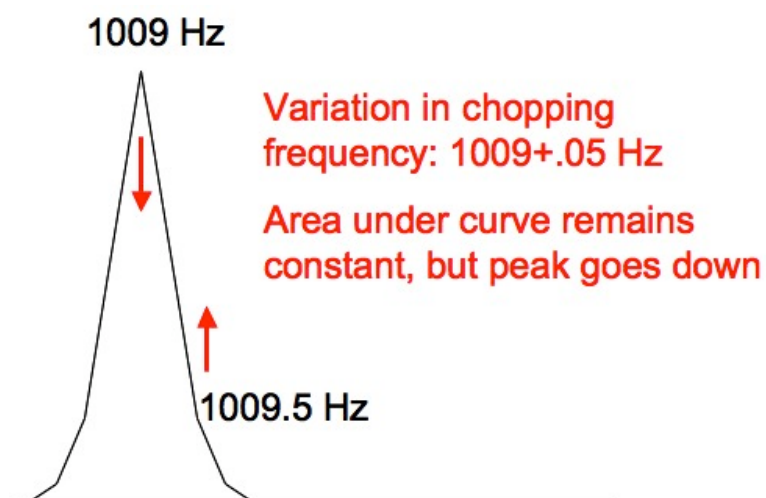


Figure 29: Example of binning problem with spectrum analyzer

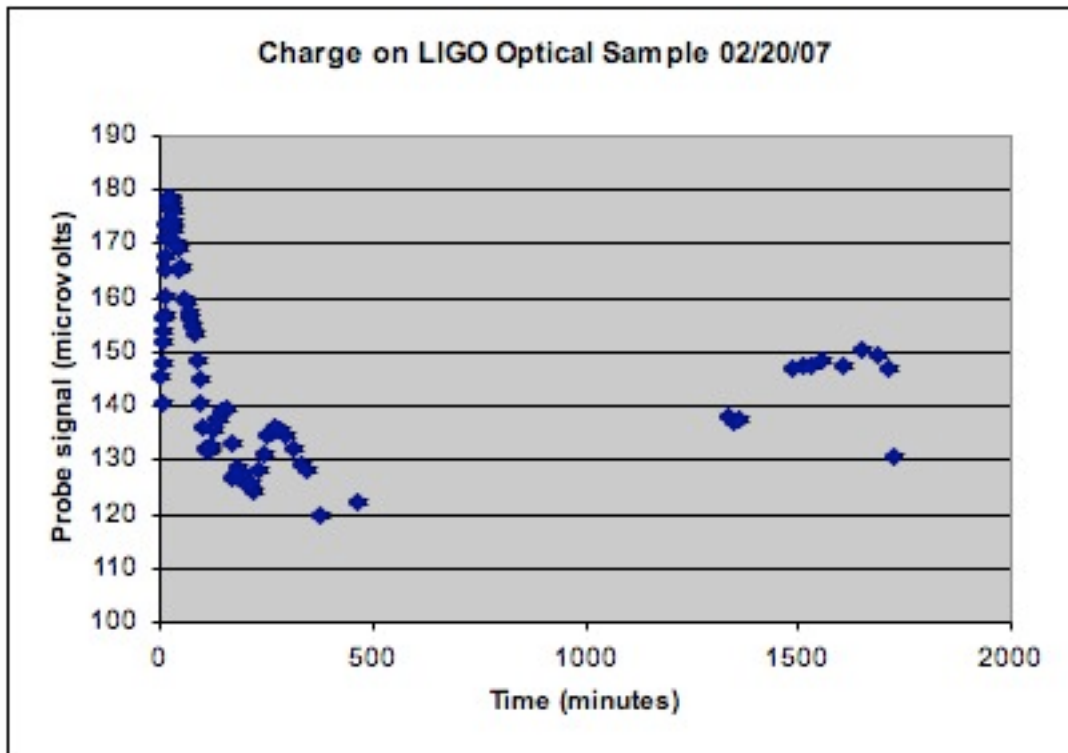


Figure 30: Signal measured on optic with spectrum analyzer

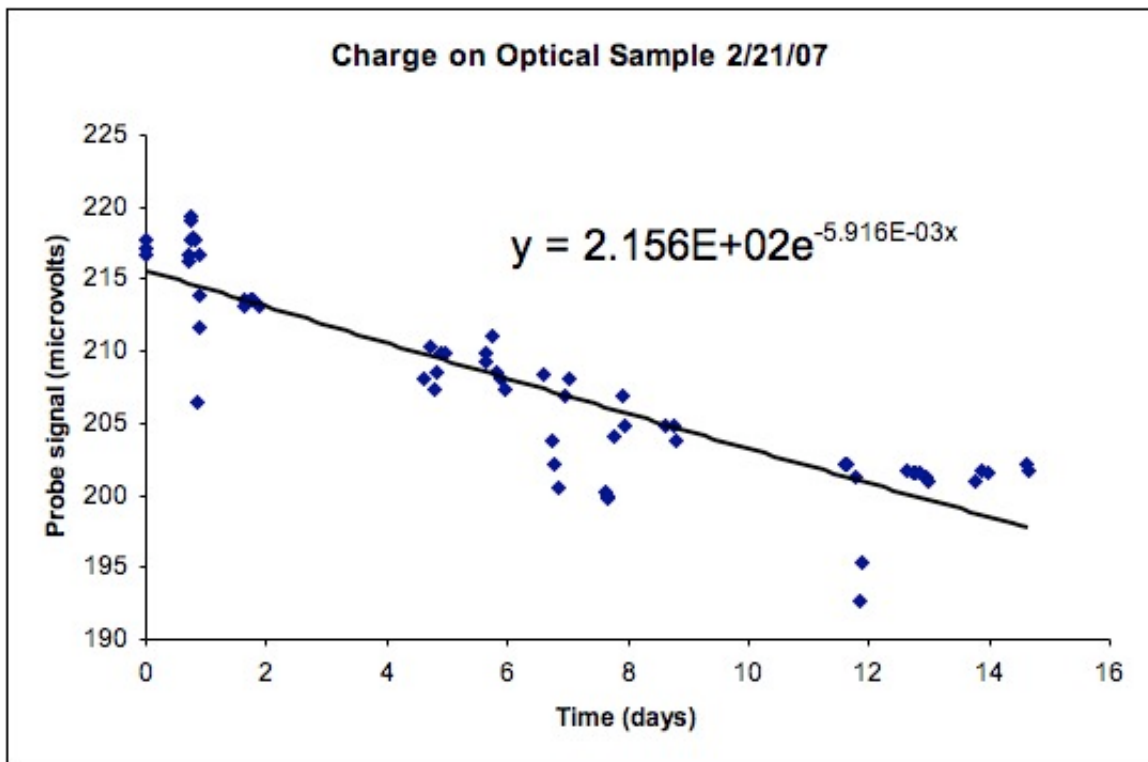


Figure 31: Signal decay over 16 day period in vacuum

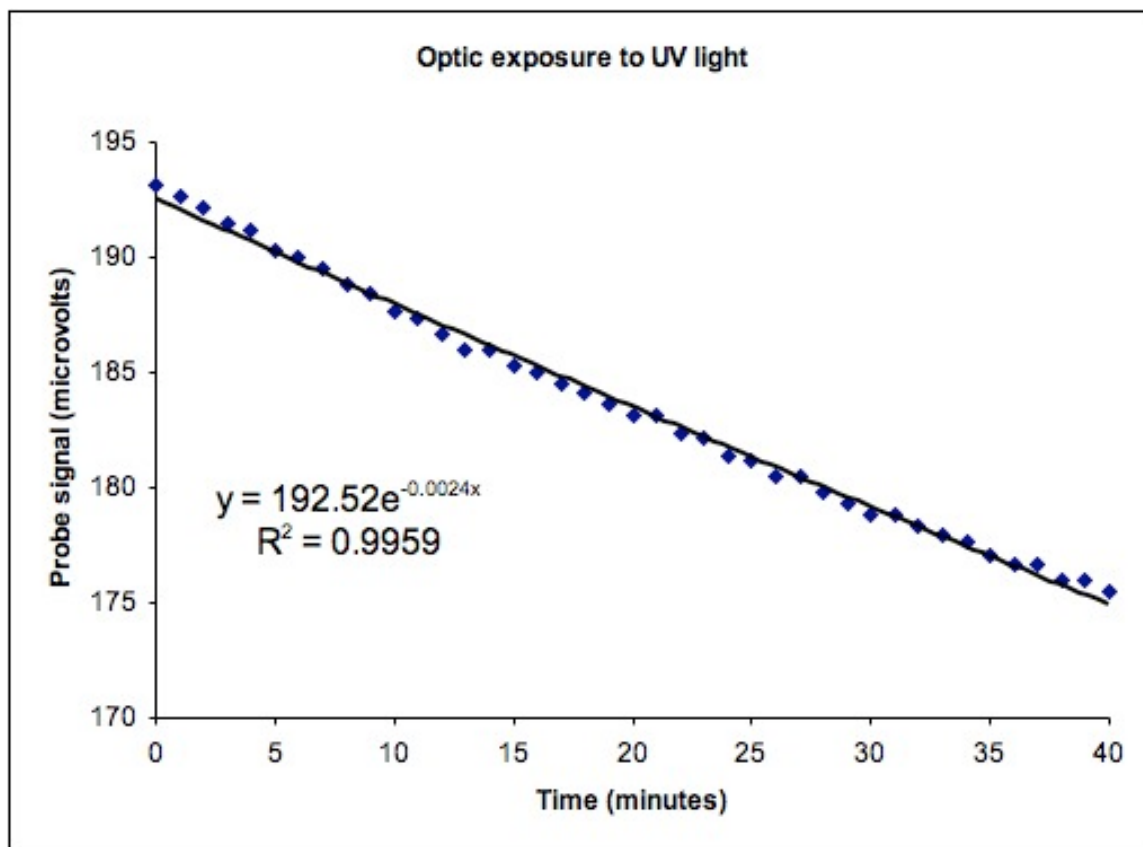


Figure 32: Optic discharge with UV light

Conclusions

The purpose of this project has been to determine if the electrostatic charging of the fused silica optics is a potential noise source in LIGO. We built a capacitive probe to measure the amount of surface charge buildup on an optic and also to measure the rate at which charge decays on the optic. Our capacitive probe achieved a sensitivity in air of $(2.3 \pm 0.3) \cdot 10^5 \text{ e}^-/\text{cm}^2$. With the probe we discovered that fused silica optics can buildup a large amount of surface charge on the order of $8 \cdot 10^7 \text{ e}^-/\text{cm}^2$, especially when rubbed with the Viton seals that are used as earthquake stops in the LIGO interferometer. Once the optic was in vacuum we found that charge decays over a long period of time on the order of hundreds of days. We discovered that some of this charge can be removed by illuminating the optic with UV light, though we did not determine whether UV light has any harmful side effects on the optical coatings. Future goals include the determination of a more precise decay constant, the different amounts of charge that can build up on the optic due to other sources of charging, and the amount of surface charge that can be removed through illumination with UV light.

Sources

- ¹ A. Abramovici *et al.* Science **256**, 325-333 (1992).
- ² B. Barish and R. Weiss. Physics Today **52** (Oct.), 44-50 (1999).
- ³ *About LIGO*. LIGO Website: http://www.ligo.caltech.edu/LIGO_web/about/
- ⁴ A. Siegman. Lasers. University Science Books. Mill Valley, CA (1986).
- ⁵ A. Douglas Davis. Classical Mechanics. Academic Press. Orlando, FL (1986).
- ⁶ J.B. Marion and S.T. Thornton. Classical Dynamics of Particles and Systems. 4th Ed. Harcourt College Publishers. Fort Worth, TX (1995).
- ⁷ R. Weiss. LIGO Internal Note: T960137-00.
- ⁸ D. Ugolini *et al.* LIGO Internal Note: T060140-00-R.
- ⁹ V.B. Braginsky. “Experiments with Probe Masses.” PNAS published 2/12/2007
10.1073/pnas.0610311104
- ¹⁰ M. Plischke and B. Bergersen. Equilibrium Statistical Physics. 2nd Ed. World Scientific. New Jersey (1994).
- ¹¹ L.D. Landau and E.M. Lifshitz. Statistical Physics. Pergamon Press Ltd. Reading, MA (1958).
- ¹² D. Ugolini, R. McKinney, and G. Harry. “Developing a Capacitive Probe for measuring surface charge on in-vacuum optics.” To be published in Rev. Sci. Instr.
- ¹³ K-X. Sun *et al.* LIGO Test Mass Charging Mitigation Using Modulated LED Deep UV Light. LIGO document G060172-00-Z (2006).
- ¹⁴ V.P. Mitrofanov, L.G. Prokhorov, and K.V. Tokmakov, Phys. Lett. A **300**, 370 (2002).
- ¹⁵ I.D. Baikie. The Kelvin Probe Information Site:
<http://www.kelvinprobe.info/index.html>
- ¹⁶ M.J. Mortonson *et al.* Effects of electrical charging on the mechanical Q of a fused silica disk. LIGO Laboratory, MIT. June 30, 2003.
- ¹⁷ D. Coyne. LIGO Vacuum Compatible Materials List. LIGO-E960050-B-E released by DCN E030570-01. 5 April 2004.
- ¹⁸ Instruction Manual to Surface DC Voltmeter, AlphaLab, Inc.